ELSEVIER

0141-1187(94)00014-X

Applied Ocean Research 16 (1994) 129–139

0141-1187/94/$07.00

Scattering of water waves by submerged curved plates and by surface-piercing flat plates

N. F. Parsons & P. A. Martin

Department of Mathematics, University of Manchester, Manchester, UK, M13 9PL

(Received 16 June 1994; revised version received and accepted 29 July 1994)

Previous work on the scattering of regular surface water waves by a single, flat, submerged plate is extended to consider the scattering by submerged, curved plates and also by surface-piercing, flat plates. Problems are again formulated as hypersingular integral equations for the discontinuity in potential across the plate, which are then solved numerically using Chebyshev expansions and collocation. New results are given for submerged plates in the shape of a circular arc, and for surface-piercing plates at small angles of inclination to the horizontal. The latter configuration supports a hitherto unsuspected quasi-resonant behaviour, with a very spiky frequency response.

1 INTRODUCTION

In a previous paper,[1] a method for studying the interaction between water waves and thin plates was developed. Two-dimensional problems were considered, in which a time-harmonic small-amplitude wave is scattered by a thin plate of infinite length. This is a basic problem in linear hydrodynamics, with applications to certain types of breakwaters; a review of the relevant literature has been made,[1] and will not be repeated here.

To solve such problems, a hypersingular boundary integral equation was derived over the plate for the unknown discontinuity in the velocity potential across the plate. To solve the integral equation, an expansion-collocation method was used, involving Chebyshev polynomials of the second kind; this method is convenient, accurate and has a firm theoretical foundation. Results are presented for scattering by submerged flat plates, these are in good agreement with the known analytical solution for vertical plates[2] and with published numerical solutions for horizontal plates,[3,4] and new results are given for inclined plates.

In the present paper, the above work is extended in two directions. First, submerged *curved* plates are considered. In principle, this is straightforward, although the details are not. Specifically, numerical results for curves that are arcs of circles are given. This enables the computations to be checked in two ways (the authors are not aware of any published results for curved plates): the plate can be deformed away from a flat plate, for which reliable results have been obtained; and the circular arc can be allowed to approach a complete circle, for which the reflection coefficient is known to vanish identically.[5,6]

Second, plates that *pierce the free surface* are considered. For simplicity, it is assumed that the plate is flat, although this assumption is not essential. For such surface-piercing barriers, the main difficulty is associated with the behaviour near the point where the plate meets the free surface. Indeed, the governing integral equation can be analysed so as to extract the allowable singularities; solutions that are bounded at the intersection point are sought, as this is consistent with Ursell's[7] exact solution for a vertical barrier. The expansion-collocation method for surface-piercing plates is adapted and good agreement with Ursell[7] is found. Also, what happens as the plate becomes horizontal is explored, so that there is a narrow wedge-shaped region above the plate: we find that the graph of reflection coefficient against frequency is composed of a series of spikes superimposed on an underlying smooth curve. The latter is identified as the reflection coefficient for a *finite dock* (plate lying *in* the free surface), whereas the spikes are clearly due to a resonance effect. It should be possible to give an asymptotic analysis of this interesting phenomenon, but this has not been pursued.

2 FORMULATION

A cartesian coordinate system is chosen, in which y is directed vertically downwards into the fluid, the

undisturbed free surface lying at $y = 0$. The z-axis is chosen perpendicular to the direction of propagation of the incident wavetrain. A thin plate Γ (in general, Γ is a finite, simple, smooth arc) lying parallel to the incident wavecrests, is introduced below the free surface of the fluid, the submergence of the plate being independent of z. The problem is assumed two-dimensional, by considering a plate infinitely long in the z-direction, and the motion is taken to be simple harmonic in time. The assumptions of an inviscid, incompressible fluid, and an irrotational motion are used, to allow the introduction of a velocity potential $\mathrm{Re}\{[\phi_{\mathrm{inc}}(x,y) + \phi_{\mathrm{sc}}(x,y)]\,\mathrm{e}^{-\mathrm{i}\omega t}\}$ to describe the small fluid motions. Here, the linearity of the problem has been used to decompose the total potential, ϕ, into the sum of the incident potential, ϕ_{inc} (the potential in the absence of the plate) and the scattered potential, ϕ_{sc} (the potential due to the presence of the plate). The known incident potential is taken throughout to be

$$\phi_{\mathrm{inc}} = \mathrm{e}^{-Ky + \mathrm{i}Kx} \tag{1}$$

where $K = \omega^2/g$ and g is the acceleration due to gravity; the potential (1) corresponds to a wave travelling towards $x = +\infty$. The scattered potential is given by the solution of the following boundary-value problem:

$$\left(\frac{\partial^2}{\partial x^2} + \frac{\partial^2}{\partial y^2}\right)\phi_{\mathrm{sc}} = 0 \qquad \text{in the fluid}$$

$$K\phi_{\mathrm{sc}} + \frac{\partial \phi_{\mathrm{sc}}}{\partial y} = 0 \qquad \text{on } y = 0, \text{ and}$$

$$\frac{\partial \phi_{\mathrm{sc}}}{\partial n} = -\frac{\partial \phi_{\mathrm{inc}}}{\partial n} \qquad \text{on } \Gamma$$

$\partial/\partial n$ is normal differentiation on Γ. In addition, ϕ_{sc} must satisfy a radiation condition at infinity.[1]

3 THE INTEGRAL EQUATION

The above general boundary-value problem can be formulated as a hypersingular integral equation for the unknown discontinuity in potential across Γ, $[\phi]$. This process has been discussed by Martin and Rizzo[8] and by Parsons and Martin.[1] The result is

$$\frac{1}{2\pi} \Xint-_{\Gamma} [\phi(q)] \frac{\partial^2 G(p,q)}{\partial n_p \partial n_q}\, \mathrm{d}s_q = -\frac{\partial \phi_{\mathrm{inc}}}{\partial n_p}, \qquad p \in \Gamma \tag{2}$$

where p and q are points on Γ, the cross on the integral indicates that it is to be interpreted as a Hadamard finite-part integral, and G is the usual fundamental solution for such problems:

$$G(p;q) \equiv G(x,y;\xi,\eta) = \ln(R/R_1) - 2\phi_0(X,Y)$$

where

$$\begin{aligned} X &= x - \xi \\ Y &= y + \eta \\ \mathbf{R} &= (x - \xi, y - \eta) \\ R &= |\mathbf{R}| \\ R_1^2 &= X^2 + Y^2 \qquad \text{and} \end{aligned} \tag{3}$$

$$\phi_0(X,Y) = \int_0^\infty \mathrm{e}^{-kY} \cos kX \frac{\mathrm{d}k}{k - K}$$

We will also need the related function

$$\Psi_0(X,Y) = \int_0^\infty \mathrm{e}^{-kY} \sin kX \frac{\mathrm{d}k}{k - K}$$

Expansions for ϕ_0 and Ψ_0, found by Yu and Ursell,[9] are convenient for their computation; these are

$$\begin{aligned} \phi_0(X,Y) = -\mathrm{e}^{-KY}\{&(\ln KR_1 - \pi\mathrm{i} + \gamma) \\ &\times \cos KX + \Theta_1 \sin KX\} \\ &+ \sum_{m=1}^{\infty} \frac{(-KR_1)^m}{m!} \\ &\times \left(\frac{1}{1} + \frac{1}{2} + \cdots + \frac{1}{m}\right) \cos m\Theta_1 \end{aligned} \tag{4}$$

$$\begin{aligned} \Psi_0(X,Y) = -\mathrm{e}^{-KY}\{&(\ln KR_1 - \pi\mathrm{i} + \gamma) \\ &\times \sin KX - \Theta_1 \cos KX\} \\ &- \sum_{m=1}^{\infty} \frac{(-KR_1)^m}{m!} \\ &\times \left(\frac{1}{1} + \frac{1}{2} + \cdots + \frac{1}{m}\right) \sin m\Theta_1 \end{aligned} \tag{5}$$

where $\Theta_1 = \tan^{-1}(X/Y)$ and $\gamma = 0{\cdot}5772\ldots$ is Euler's constant.

For both problems looked at (submerged curved plates in Section 4 and surface-piercing plates in Section 5), the governing integral equation is eqn (2), the only difference being the behaviour of the unknown function, $[\phi]$, at the ends of the plate. Thus, the kernel, $\partial^2 G/\partial n_p \partial n_q$, remains the same and is given by[1]

$$\begin{aligned} \frac{\partial^2 G}{\partial n_p \partial n_q} = &-\frac{\mathcal{N}}{R^2} + \frac{2\Theta}{R^4} \\ &+ 2(n_1^p n_2^q - n_2^p n_1^q)\left\{K\frac{\partial \phi_0}{\partial X} - \frac{XY}{(X^2+Y^2)^2}\right\} \\ &- \mathcal{N}\mathcal{K}(X,Y) \end{aligned} \tag{6}$$

where

$$\mathcal{K}(X,Y) = \frac{Y^2 - X^2}{(X^2+Y^2)^2} + \frac{2KY}{X^2+Y^2} + 2K^2\phi_0(X,Y) \tag{7}$$

$\mathcal{N} = \mathbf{n}(p)\cdot\mathbf{n}(q)$ and $\Theta = (\mathbf{n}(p)\cdot\mathbf{R})(\mathbf{n}(q)\cdot\mathbf{R})$, with $\mathbf{n}(p)$

and $\mathbf{n}(q)$ denoting the unit normals at p and q, respectively.

4 THE SUBMERGED, CURVED PLATE

The geometry is given in Fig. 1. The problem is formulated in terms of b, d and ϑ; the plate length is $2a = 2b\vartheta$. From Fig. 1, we can see that a suitable parametrisation for $q \equiv (\xi, \eta)$ on Γ is

$$\xi(t) = b \sin t\vartheta \quad \eta(t) = d + b - b\cos t\vartheta \quad -1 \le t \le 1 \tag{8}$$

where $|\vartheta| < \pi$ and d is the submergence of the mid-point of the plate; the point $p \equiv (x, y)$ on Γ has the same parametrisation as eqn (8) but with t replaced by s. We introduce the function $f(t) \equiv [\phi(q(t))]$ and construct the kernel defined by eqn (6). Using the above parametrisation, we have

$$\begin{aligned}
X &= b(\sin s\vartheta - \sin t\vartheta) \\
Y &= 2d + 2b - b(\cos s\vartheta + \cos t\vartheta) \qquad (9) \\
\mathbf{n}(p) &= (n_1^p, n_2^p) = (-\sin s\vartheta, \cos\vartheta) \\
\mathbf{n}(q) &= (n_1^q, n_2^q) = (-\sin t\vartheta, \cos t\vartheta) \\
\mathcal{N} &= \cos(s-t)\vartheta \\
n_1^p n_2^q - n_2^p n_1^q &= -\sin(s-t)\vartheta \\
\mathbf{R} &= b(\sin s\vartheta - \sin t\vartheta, \cos t\vartheta - \cos s\vartheta) \\
\Theta &= -b^2[1-\cos(s-t)\vartheta]^2 \\
R^2 &= 2b^2[1-\cos(s-t)\vartheta]
\end{aligned}$$

From eqn (6), we see that the singular terms must come from the first two terms on the right-hand side. Thus, writing $h = (s-t)\vartheta/2$, we have

$$\begin{aligned}
-\frac{\mathcal{N}}{R^2} + \frac{2\Theta}{R^4} &= -\frac{\cos 2h}{2b^2(1-\cos 2h)} - \frac{1}{2b^2} \\
&= -\frac{1}{4b^2\sin^2 h} \qquad (10) \\
&\approx -\frac{1}{4b^2h^2}\left(1 + \frac{h^2}{3} + \frac{h^4}{15} + \frac{2h^6}{189} + \cdots\right) \qquad (11)
\end{aligned}$$

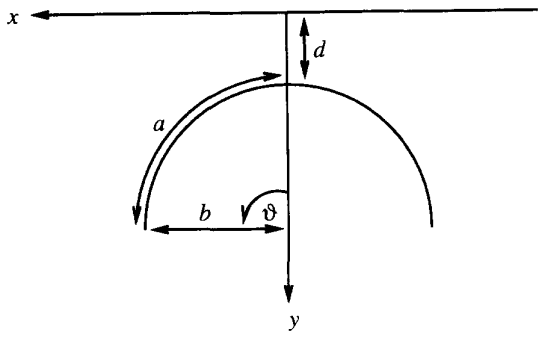

Fig. 1. Geometry of the submerged, curved plate.

as $h \to 0$. Equation (10) shows that a double pole exists as $s = t$, which is characteristic of simple hypersingular kernels. Equation (11) gives a local expansion near the singularity. For computational purposes, we extract the hypersingularity and write

$$\begin{aligned}
-\frac{\mathcal{N}}{R^2} + \frac{2\Theta}{R^4} &= -\frac{1}{b^2\vartheta^2(s-t)^2} \\
&\quad - \frac{1}{4b^2}\left(\frac{1}{\sin^2[(s-t)\vartheta/2]} - \frac{4}{(s-t)^2\vartheta^2}\right) \\
&\approx -\frac{1}{b^2\vartheta^2(s-t)^2} \\
&\quad - \frac{1}{4b^2}\left(\frac{1}{3} + \frac{(s-t)^2\vartheta^2}{60} + \frac{(s-t)^4\vartheta^4}{1512}\right) \qquad (12)
\end{aligned}$$

neglecting terms of $O((s-t)^6\vartheta^6)$. Equation (2) can now be written in the parametrised form

$$\int\!\!\!\!\!\!^{\,1}_{-1} \frac{f(t)}{(s-t)^2}\,\mathrm{d}t + \int_{-1}^{1} f(t)K(s,t)\,\mathrm{d}t = v(s) \quad -1 < s < 1 \tag{13}$$

where

$$\begin{aligned}
K(s,t) &= \frac{\vartheta^2}{4}\left(\frac{1}{\sin^2[(s-t)\vartheta/2]} - \frac{4}{(s-t)^2\vartheta^2}\right) \\
&\quad + 2b^2\vartheta^2\left\{K\frac{\partial\phi_0}{\partial X} - \frac{XY}{(X^2+Y^2)^2}\right\} \\
&\quad \times \sin[(s-t)\vartheta] + b^2\vartheta^2\mathcal{K}(X,Y)\cos[(s-t)\vartheta] \\
v(s) &= -2\pi b\vartheta K\,\mathrm{e}^{-Kd+\mathrm{i}s\vartheta}\exp[-Kb(1-\mathrm{e}^{\mathrm{i}s\vartheta})]
\end{aligned}$$

X and Y are given by eqn (9), and the property $\mathrm{d}s_q = b\vartheta\,\mathrm{d}t$ has been used. The hypersingular term has thus been separated from the regular terms. It will now be shown how this is advantageous when solving eqn (13).

4.1 Numerical solution

To solve eqn (13), we start by approximating $f(t)$ as follows:

$$f(t) \cong \sqrt{1-t^2}\sum_{n=0}^{N} a_n U_n(t) \tag{14}$$

where $U_n(t)$ is a Chebyshev polynomial of the second kind and the unknown coefficients, a_n, are to be found; the square-root factor ensures that $f(t)$ has the correct behaviour at each end of the plate, where the potential vanishes.[10] Without going into too much detail, the unknown coefficients can be found by either a classical Galerkin method, or a more straightforward collocation scheme; the latter approach is adopted here. Thus, first of all replace $f(t)$ in eqn (13) by the expansion (14)

giving

$$\sum_{n=0}^{N} a_n A_n(s) = v(s) \qquad -1 < s < 1$$

where

$$A_n(s) = \int\!\!\!\!\!\!-_{-1}^{1} \frac{\sqrt{1-t^2}U_n(t)}{(s-t)^2}\,\mathrm{d}t + \int_{-1}^{1} \sqrt{1-t^2}U_n(t)K(s,t)\,\mathrm{d}t$$

and then collocate at $s_j, j = 0, 1, \ldots, N$. A suitable set of collocation points is given by

$$s_j = \cos\left(\frac{(2j+1)\pi}{2N+2}\right) \qquad j = 0, 1, \ldots, N \tag{15}$$

these being the zeros of $T_{N+1}(s)$ (a Chebyshev polynomial of the first kind). Golberg[11,12] has shown that the above scheme is uniformly convergent; he and Ervin and Stephan[13] have also analysed other choices for the collocation points. An important aspect of this approach is that it allows the hypersingular integration to be done analytically. Thus, it can be shown that[1]

$$\int\!\!\!\!\!\!-_{-1}^{1} \frac{\sqrt{1-t^2}U_n(t)}{(s-t)^2}\,\mathrm{d}t = -\pi(n+1)U_n(s)$$

The remaining terms on the left-hand side of eqn (13) can be integrated numerically, where, for small $|s-t|\vartheta$, eqn (12) is used. The only slight problem concerns the term $\partial\phi_0/\partial X$. This is treated as follows. From eqn (3), we have

$$\begin{aligned}\frac{\partial\phi_0}{\partial X} &= -\int\!\!\!\!\!\!-_0^{\infty} k\,\mathrm{e}^{-kY}\sin kX\,\frac{\mathrm{d}k}{k-K} \\ &= -\int\!\!\!\!\!\!-_0^{\infty} (k-K+K)\,\mathrm{e}^{-kY}\sin kX\,\frac{\mathrm{d}k}{k-K} \\ &= -\frac{X}{X^2+Y^2} - K\Psi_0(X,Y)\end{aligned}$$

where Ψ_0 can be evaluated using eqn (5).

4.2 Results

As an example of the efficacy of the above method, the reflection and transmission coefficients were computed. Consider the reflection coefficient, $\mathscr{R}$. It can be shown that $\mathscr{R}$ has the integral representation[1]

$$\mathscr{R} = -\mathrm{i}\int_\Gamma [\phi(q)]\,\frac{\partial}{\partial n_q}\,\mathrm{e}^{-K\eta+\mathrm{i}K\xi}\,\mathrm{d}s_q \tag{16}$$

So, differentiating normally at q, and using the parametrisation (8), we obtain

$$\mathscr{R} = \mathrm{i}Kb\vartheta\,\mathrm{e}^{-K(d+b)}\int_{-1}^{1} f(t)\exp\left[Kb\,\mathrm{e}^{\mathrm{i}t\vartheta} + \mathrm{i}t\vartheta\right]\mathrm{d}t \tag{17}$$

Replacing $f(t)$ in eqn (17) by its Chebyshev expansion (14), we find that

$$\mathscr{R} \cong \mathrm{i}Kb\vartheta\,\mathrm{e}^{-K(d+b)}\sum_{n=0}^{N} a_n F_n$$

where

$$F_n = \int_{-1}^{1} \sqrt{1-t^2}U_n(t)\exp\left[Kb\,\mathrm{e}^{\mathrm{i}t\vartheta} + \mathrm{i}t\vartheta\right]\mathrm{d}t$$

A similar procedure can be applied to the transmission coefficient, $\mathscr{T}$, giving

$$\mathscr{T} \cong 1 + \mathrm{i}Kb\vartheta\,\mathrm{e}^{-K(d+b)}\sum_{n=0}^{N} a_n\overline{F_n}$$

where the overbar denotes complex conjugation. The integral F_n can easily be evaluated numerically after making the substitution $t = \cos\psi$.

For our first results, we choose to plot $|\mathscr{R}|$ against Ka for various ϑ. Figure 2 shows graphs of $|\mathscr{R}|$ (where $d/a = 0{\cdot}1$) for $\vartheta = \pi/10$, $2\pi/10$ and also for the flat plate corresponding to letting $\vartheta \to 0$ whilst keeping a non-zero. We can see that the transition from the horizontal plate to the curved plate is similar to that seen for an angled plate,[1] inasmuch as there are abrupt changes in the value of $|\mathscr{R}|$ for small changes in ϑ. However, whereas the zeros of $\mathscr{R}$ vanish immediately for the angled plate, it can be seen that (numerically, at least) the zeros for the curved plate in this configuration remain, albeit shifted towards the right with increasing ϑ.

In Figures 3 and 4, we continue to increase ϑ (for the same value of d/a), thereby approaching the geometry of a closed circular cylinder. We see that $|\mathscr{R}|$ almost vanishes in this limit, for *all* frequencies. This behaviour is expected, as Dean[5] first showed that $\mathscr{R} \equiv 0$ for a submerged circular cylinder at *any* frequency. This result was subsequently proved by Ursell,[6] using a rigorous argument.

Similar results have been obtained for $d/a = 0{\cdot}2$;[14] as expected, a general reduction in $|\mathscr{R}|$ was found throughout the frequency range, due to the deeper submergence.

The previous results can be thought of as fixing the length of the plate, whilst varying ϑ, thereby bending the plate until it creates a circular cylinder. However, due to the many parameters in this problem, the radius b can also be fixed, and then ϑ can be varied. Thus, the plate length increases and also closes up to a circular cylinder as ϑ is increased. Figure 5 contains graphs of $|\mathscr{R}|$ against Kb for $d/b = 0{\cdot}1$ and various values of ϑ. Again, we see that the zeros of $\mathscr{R}$ remain, this time shifted to the left with increasing ϑ. The peak values of $|\mathscr{R}|$ all reduce with increasing ϑ and also become shifted to the left. As with the previous results, onset of zero reflection is noticed as the plate approaches a complete circle. Figure 6 contains similar results with $d/b = 0{\cdot}2$. This time, the graph for

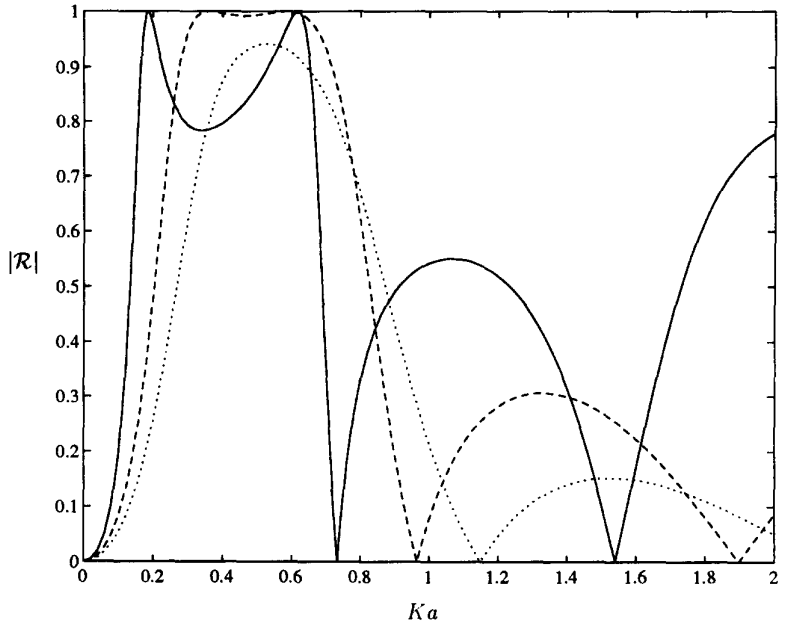

Fig. 2. Graphs of $|\mathcal{R}|$ against Ka, where $d/a = 0{\cdot}1$, for $\vartheta = \pi/10$ (– –), $2\pi/10$ ($\cdots$) and also the flat plate limit; that is, where $\vartheta \to 0$ keeping a non-zero (—).

$\vartheta = \pi/8$ has a lower peak of $|\mathcal{R}|$ than the graph for $\vartheta = 2\pi/8$, thereafter they follow the same pattern as Fig. 5.

5 THE SURFACE-PIERCING, FLAT PLATE

In this section, the more difficult problem of scattering by a surface-piercing, flat plate is studied. The authors are aware of only a few papers on this problem when the plate is not vertical. Thus, John[15] gave a complex-function analysis for plates making an angle of $\pi/2n$ to the horizontal, where n is an integer, although he did not give explicit results (even when $n = 2$). Liu and Abbaspour[16] have used a simple boundary integral equation method for water of finite depth; their method does not account for the plate-edge singularities in a natural way (special elements are used). Finally, Hamilton[17] has given some experimental results for plates at small inclinations to the horizontal.

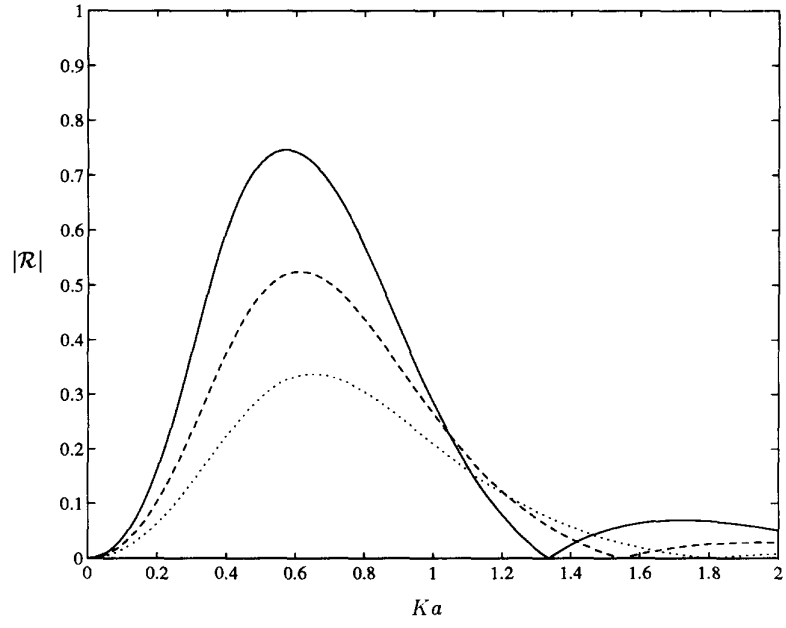

Fig. 3. Graphs of $|\mathcal{R}|$ against Ka, where $d/a = 0{\cdot}1$, for $\vartheta = 3\pi/10$ (—), $4\pi/10$ (– –) and $5\pi/10$ ($\cdots$).

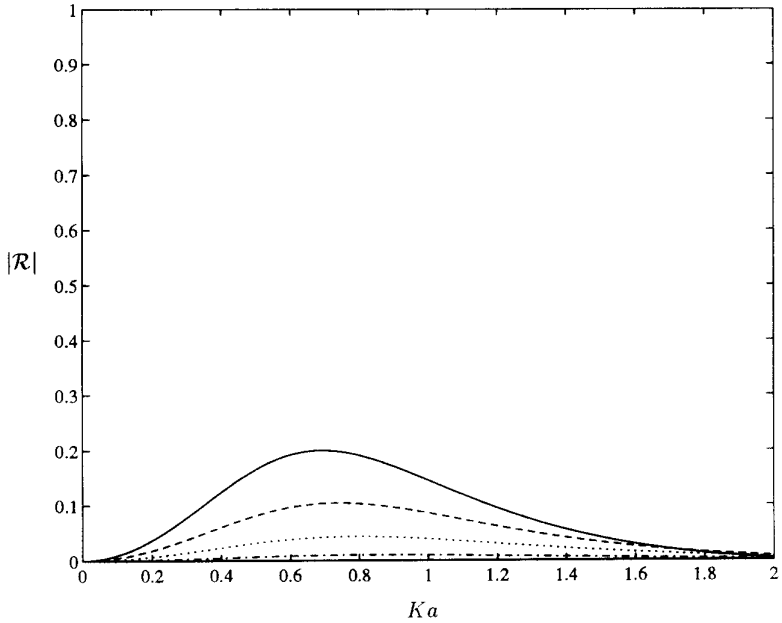

Fig. 4. Graphs of $|\mathscr{R}|$ against Ka, where $d/a = 0{\cdot}1$, for $\vartheta = 6\pi/10$ (—), $7\pi/10$ (– –), $8\pi/10$ (· · ·) and $9\pi/10$ (– ·).

As in Section 4, the problem is governed by the hypersingular integral equation for the discontinuity in potential across the plate, eqn (2). This time, the expected square-root zero in discontinuity at the submerged end of the plate is retained. However, where the plate meets the free surface, there is more ambiguity. For example, it may be possible to permit a logarithmic singularity in discontinuity at the free surface. This may be used as a model for wave breaking.[18] This course will not be pursued here, but it will be assumed that the discontinuity approaches a constant as the free surface is approached; this is in accord with the exact solution of Ursell[7] for a vertical plate.

Having formulated the problem, an identical expansion is used for the discontinuity in potential across the plate as that used previously for submerged plates:

$$f(t) \cong \sqrt{1-t^2} \sum_{n=0}^{N} a_n U_n(t) \tag{18}$$

where $f(t)$ is the discontinuity in potential across the

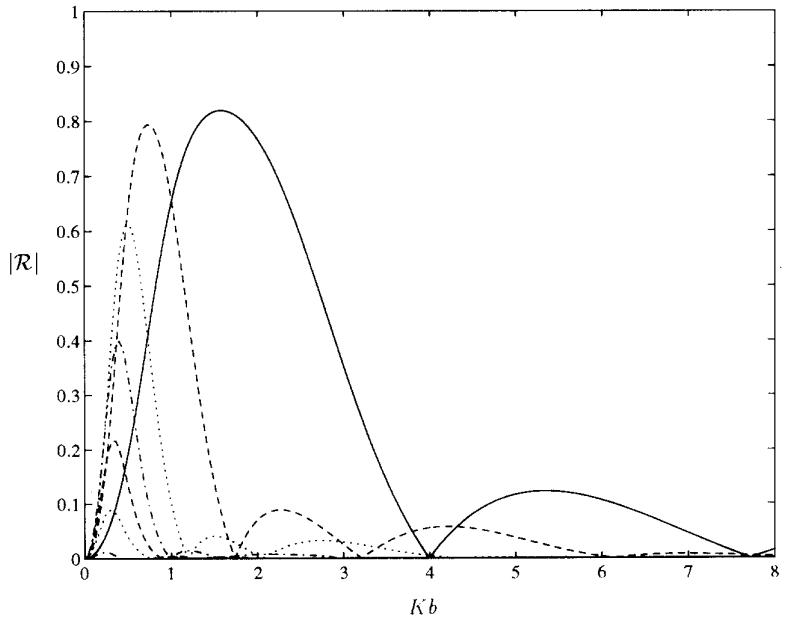

Fig. 5. Graphs of $|\mathscr{R}|$ against Kb, where $d/b = 0{\cdot}1$, for $\vartheta = M\pi/8$ and $M = 1, 2, 3, 4, 5, 6, 7$ and 8. The graph for $\pi/8$ is given by —; thereafter the peaks of $|\mathscr{R}|$ decrease with increasing ϑ.

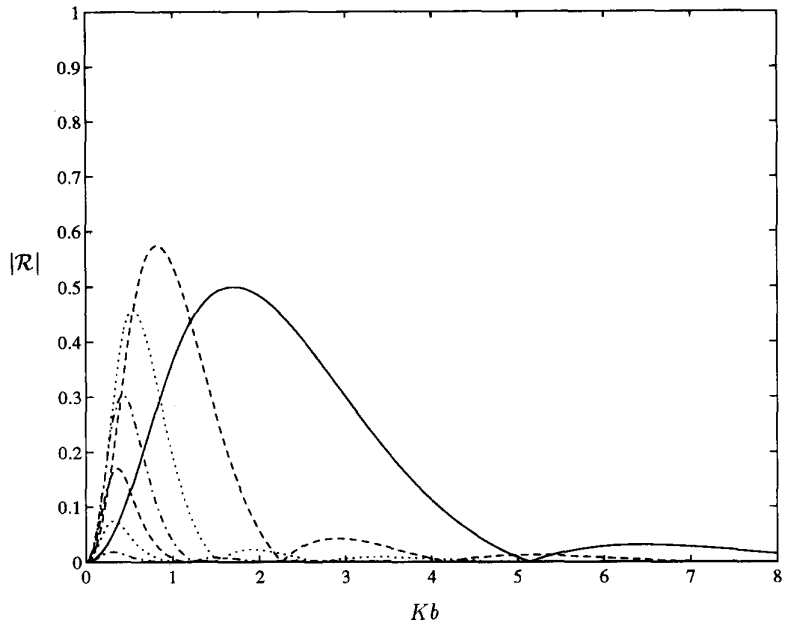

Fig. 6. Graphs of $|\mathscr{R}|$ against Kb, where $d/b = 0{\cdot}2$, for $\vartheta = M\pi/8$ and $M = 1, 2, 3, 4, 5, 6, 7$ and 8. The graph for $\pi/8$ is given by —; thereafter the peaks of $|\mathscr{R}|$ decrease with increasing ϑ.

plate, and $t = 1$ corresponds to the submerged end of the plate, with $f(1) = 0$. This time, however, the problem is parametrised in such a way that the edge of the plate piercing the free surface corresponds to the point $t = 0$, thereby giving f the constant value

$$f(0) \cong \sum_{n=0}^{[N/2]} a_{2n}(-1)^n$$

where $[x]$ represents the integer part of x. Moreover, it is known that, for a plate of unit length, $f(t)$ has the asymptotic expansion[14]

$$f(t) \sim f_0(1 - Kt\sec\theta) + f_\delta t^\delta + \tfrac{1}{4}f_0K^2t^2\sec^2\theta \quad \text{as } t \to 0 \tag{19}$$

where f_0 and f_δ are constants, $\delta = 2\pi/(\pi + 2\theta)$ and θ is the angle between the plate and the vertical. The approximation (19) was derived for $|\theta| < \pi/2$, $\theta \neq 0$; for $\theta = 0$ (the vertical plate) we have[10]

$$f(t) \sim f_0(1 - Kt) + (2/\pi)(Kv_0 + v_1)t^2\ln t + f_2t^2 \quad \text{as } t \to 0$$

where f_0, v_0, v_1 and f_2 are all constants. In the same paper,[10] it is shown that for a problem involving a regular incident wave (such as eqn (1)), the term $Kv_0 + v_1$ is identically zero. We will soon see the significance of these properties.

5.1 The kernel

The geometry of the problem is shown in Fig. 7, whence a suitable parametrisation is given by

$$\xi(t) = a(2t - 1)\sin\theta, \quad \eta(t) = 2at\cos\theta, \quad 0 \le t \le 1 \tag{20}$$

where $2a$ is the length of the plate, $q \equiv (\xi, \eta)$, $|\theta| < \pi/2$ and $t = 0$ corresponds to the free surface. The restriction on θ prevents the plate from lying *in* the free surface. The problem of scattering by a plate lying in the free surface is known as the *dock problem*. The point $p \equiv (x, y)$ on the plate has the same parametrisation as q, but with t replaced by s. With this parametrisation, we find that eqn (2) can be written as

$$\oint_0^1 \frac{f(t)}{(s-t)^2}\,\mathrm{d}t + 4a^2\int_0^1 f(t)\mathscr{K}(X, Y)\,\mathrm{d}t = v(s) \quad 0 < s < 1 \tag{21}$$

where $\mathscr{K}$ is defined by eqn (7), $X = 2a(s - t)\sin\theta$, $Y = 2a(s + t)\cos\theta$ and

$$v(s) = 8\pi Ka\exp[-2Kas\cos\theta + \mathrm{i}(Ka(2s - 1)\sin\theta - \theta - \pi/2)] \tag{22}$$

Again, we have separated the hypersingular term from the regular terms. Before proceeding with the

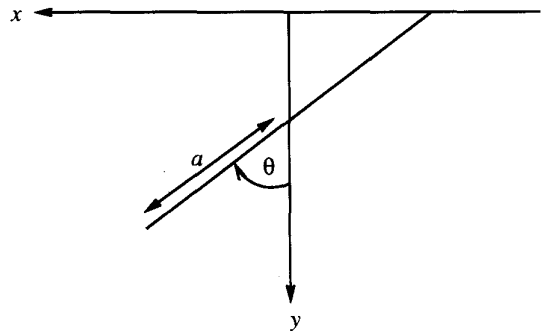

Fig. 7. Geometry of the surface-piercing, flat plate.

numerical solution, we obtain a useful simplification of $\mathscr{K}(X, Y)$. Thus, considering the first term of $\mathscr{K}(X, Y)$, we have

$$\frac{a^2(Y^2 - X^2)}{(X^2 + Y^2)^2} = \frac{1}{4}\left\{\frac{(s^2 + t^2)\cos 2\theta + 2st}{(s^2 + t^2 + 2st\cos 2\theta)^2}\right\}$$
$$= \frac{1}{8}\left\{\frac{e^{-2i\theta}}{(se^{-2i\theta} + t)^2} + \frac{e^{2i\theta}}{(se^{2i\theta} + t)^2}\right\} \quad (23)$$

where we have used $s^2 + t^2 + 2st\cos 2\theta = (s + te^{2i\theta})\times(s + te^{2i\theta})$ and a partial fraction expansion. Similarly, the second term in $\mathscr{K}(X, Y)$ is proportional to

$$\frac{4aY}{X^2 + Y^2} = \frac{2(s + t)\cos\theta}{s^2 + t^2 + 2st\cos 2\theta}$$
$$= \frac{e^{-i\theta}}{se^{-2i\theta} + t} + \frac{e^{i\theta}}{se^{2i\theta} + t} \quad (24)$$

Using eqns (23) and (24), eqn (21) can be written as

$$\int\!\!\!\!\!\!-_0^1 \frac{f(t)}{(s - t)^2}\,dt + \frac{e^{2i\theta}}{2}\int_0^1 \frac{f(t)}{(z + t)^2}\,dt$$
$$+ \frac{e^{-2i\theta}}{2}\int_0^1 \frac{f(t)}{(\bar{z} + t)^2}\,dt + 2Kae^{i\theta}\int_0^1 \frac{f(t)}{z + t}\,dt$$
$$+ 2Kae^{-i\theta}\int_0^1 \frac{f(t)}{\bar{z} + t}\,dt$$
$$+ 8(Ka)^2\int_0^1 f(t)\phi_0(X, Y)\,dt = v(s) \quad (25)$$

where $v(s)$ is defined by eqn (22), $z = se^{2i\theta}$ and $\bar{z} = se^{-2i\theta}$. In view of the restriction on $\theta(|\theta| < \pi/2)$, we see that $-\pi < \arg z < \pi$. From eqn (25), as we collocate towards the free surface, the four integrals involving z and $\bar{z}$ become singular. This causes two problems in the analysis. First, keeping all our computations as accurate as possible requires an efficient method of calculating the integrals which become singular in eqn (25). Fortunately, this is possible by using recurrence relations for the integrals which will be discussed shortly. Secondly, it is noticed that the right-hand side of the integral equation, $v(s)$, is perfectly well behaved for all s, even $s = 0$. However, the left-hand side of the integral equation appears to be singular at $s = 0$. The explanation for this is that $f(t)$ has a particular behaviour as $t \to 0$ to ensure that the left-hand side of eqn (25) remains bounded for all s. Indeed, taking a model problem where $f(t)$ is given by (cf. eqn (19))

$$f(t) = f_0(1 - 2Kat\sec\theta) \quad (26)$$

the hypersingular integral and the four integrals which become singular as $s \to 0$ can be integrated analytically, from which it can be shown that the ratio of the constant term to the coefficient of the t-term in eqn (26) is exactly what is needed to remove any singularities in the resulting expression. This gives some explanation as to why the asymptotic expansion of $f(t)$ contains a degree of dependence between the coefficients.

Much thought has been given to the best way of dealing with this problem. For instance, is it possible to use the known behaviour of $f(t)$, eqn (19), in the solution of the problem? This would give a set of constraints to be imposed on the unknown coefficients in any Chebyshev expansion used. This, however, changes the behaviour of the solution away from the point $t = 0$, and as such is unsatisfactory. In practice, it was decided not to try and impose any restriction on $f(t)$, other than the square-root behaviour at $t = 1$ and the boundedness at $t = 0$. It turns out that this approach is simple and effective, probably because the singularity is rather weak (its effects are captured adequately by the expansion-collocation procedure). It can also be justified, in part, by its ability to recover the solution for the vertical plate given by Ursell.[7] Also, as θ is increased towards $\pi/2$, we expect to find some similarity between our solution and that for scattering by a finite dock.

5.2 Method of solution

As already stated, an expansion-collocation method is employed. Thus, we substitute the expansion (18), for $0 < t < 1$, into eqn (21) to give

$$\sum_{n=0}^{N} a_n A_n(s) = v(s) \qquad 0 < s < 1$$

where $v(s)$ is given by eqn (22),

$$A_n(s) = \mathscr{L}_n(s) + \tfrac{1}{2}e^{2i\theta}\mathscr{L}_n(-z) + \tfrac{1}{2}e^{-2i\theta}\mathscr{L}_n(-\bar{z})$$
$$- 2Kae^{i\theta}\mathscr{I}_n(-z) - 2Kae^{-i\theta}\mathscr{I}_n(-\bar{z})$$
$$+ 8(Ka)^2\int_0^1 \sqrt{1 - t^2}U_n(t)\phi_0(X, Y)\,dt \quad (27)$$

$$\mathscr{I}_n(z) = \int_0^1 \frac{\sqrt{1 - t^2}U_n(t)}{z - t}\,dt \quad (28)$$

$$\mathscr{L}_n(z) = \int\!\!\!\!\!\!-_0^1 \frac{\sqrt{1 - t^2}U_n(t)}{(z - t)^2}\,dt \quad (29)$$

and $z = se^{2i\theta}$ with $|\theta| < \pi/2$; note that the integrals (28) and (29) are non-singular except when z lies in the range of integration.

We evaluate the integrals (28) and (29) using recurrence relations which are readily derived from a known recurrence relation for $U_n(t)$. Thus,

$$\mathscr{I}_{n+1} = -\mathscr{I}_{n-1} + 2z\mathscr{I}_n - \left(\frac{1}{n} + \frac{1}{n+2}\right)\sin\left(\frac{n\pi}{2}\right)$$

for $n \geq 1$

where $\mathscr{I}_1 = 2z\mathscr{I}_0 - \frac{1}{2}\pi$ and

$$\mathscr{I}_0 = 1 + \frac{z\pi}{2} + \sqrt{1 - z^2}\ln\left(\frac{z}{1 + \sqrt{1 - z^2}}\right)$$

Similarly, $\mathscr{L}_n$ can be determined from $\mathscr{I}_n$, using

$$\mathscr{L}_{n+1} = -\mathscr{L}_{n-1} + 2z\mathscr{L}_n - 2\mathscr{I}_n \qquad \text{for } n \geq 1$$

with $\mathscr{L}_1 = 2z\mathscr{L}_0 - 2\mathscr{I}_0$ and

$$\mathscr{L}_0 = -\frac{\pi}{2} + \frac{z}{\sqrt{1-z^2}} \ln\left(\frac{z}{1+\sqrt{1-z^2}}\right) - \frac{1}{z}$$

The remaining integral in eqn (27) is well behaved as $s \to 0$, and is evaluated using the expansion for $\phi_0(X, Y)$, eqn (4). All, bar one, of the integrals arising from this substitution must be evaluated numerically. The exception is

$$\int_0^1 \sqrt{1-t^2}\, U_n(t)\, \mathrm{e}^{-2Ka(s+t)\cos\theta} \cos\left[2Ka(s-t)\sin\theta\right] \mathrm{d}t$$

$$= \mathrm{Re}\left\{ \exp\left[-2Kas\,\mathrm{e}^{-\mathrm{i}\theta}\right] \times \int_0^1 \sqrt{1-t^2}\, U_n(t) \exp\left[-2Kat\,\mathrm{e}^{\mathrm{i}\theta}\right] \mathrm{d}t \right\} \qquad (30)$$

A similar integral occurs in Section 5.3 below. We find that the first integral in eqn (30) is equal to

$$\tfrac{1}{2}\,\mathrm{Re}\left\{\exp\left[-2Kas\,\mathrm{e}^{-\mathrm{i}\theta}\right](M_n(Ka) - M_{n+2}(Ka))\right\}$$

where $M_n(K)$ is given by eqn (31).

It remains to specify the collocation points. Earlier in the paper, the collocation points s_j defined by eqn (15) were used; these points lie in the range $-1 < s_j < 1$. Now, we require collocation points in the range $0 < s_j < 1$. Therefore, we apply the simple transformation $s_j \to (s_j + 1)/2$ to eqn (15), giving us the points

$$s_j = \frac{1}{2}\left\{\cos\left(\frac{(2j+1)\pi}{2N+2}\right) + 1\right\} \qquad j = 0, 1, \ldots, N$$

With this choice, we obtain the linear system of equations

$$\sum_{n=0}^{N} a_n A_n(s_j) = v(s_j) \qquad j = 0, 1, \ldots, N$$

which is to be solved for the unknown coefficients, a_n.

5.3 Results

For the surface-piercing plate, the same formulation for the evaluation of the reflection and transmission coefficients can be used as in Section 4. Thus, $\mathscr{R}$ is given by eqn (16), which, after using the parametrisation eqn (20), becomes

$$\mathscr{R} = -Ka\,\mathrm{e}^{-\mathrm{i}(Ka\sin\theta+\theta)} \int_0^1 f(t) \exp\left[-2Kat\,\mathrm{e}^{-\mathrm{i}\theta}\right] \mathrm{d}t$$

Hence, using the Chebyshev expansion for $f(t)$,

$$\mathscr{R} \cong -Ka\,\mathrm{e}^{-\mathrm{i}(Ka\sin\theta+\theta)} \sum_{n=0}^{N} a_n \bar{h}_n(Ka)$$

where

$$h_n(K) = \int_0^1 \sqrt{1-t^2}\, U_n(t) \exp\left[-2Kt\,\mathrm{e}^{\mathrm{i}\theta}\right] \mathrm{d}t$$

Similarly, the transmission coefficient, $\mathscr{T}$, is given by

$$\mathscr{T} \cong 1 + Ka\,\mathrm{e}^{\mathrm{i}(Ka\sin\theta+\theta)} \sum_{n=0}^{N} a_n h_n(Ka)$$

We can evaluate h_n analytically. Substituting $t = \cos\psi$ gives

$$h_n(K) = \tfrac{1}{2}(M_n - M_{n+2})$$

where

$$M_n(K) = \int_0^{\pi/2} \exp\left[-2K\,\mathrm{e}^{\mathrm{i}\theta}\cos\psi\right] \cos n\psi \,\mathrm{d}\psi$$

Expanding the exponential,[19] we obtain

$$M_n(K) = \sum_{m=0}^{\infty} \epsilon_m (-1)^m I_m(2K\,\mathrm{e}^{\mathrm{i}\theta}) C_{mn} \qquad (31)$$

where $\epsilon_0 = 1$, $\epsilon_m = 2$ for $m \geq 1$ and I_m is a modified Bessel function; the coefficients, C_{mn}, are given by

$$C_{mn} = \int_0^{\pi/2} \cos m\psi \cos n\psi \,\mathrm{d}\psi$$

and are easily evaluated: $C_{00} = \pi/2$, $C_{nn} = \pi/4$ for $n > 0$, and

$$C_{mn} = \frac{1}{2}\left(\frac{\sin\left[(n-m)\pi/2\right]}{n-m} + \frac{\sin\left[(n+m)\pi/2\right]}{n+m}\right)$$

when $n \neq m$

Figure 8 shows graphs of $|\mathscr{R}|$ plotted against Ka, for the surface-piercing plate at $\theta = M\pi/12$, $M = 0, 1, 2, 3, 4$ and 5, to the vertical. The case $M = 0$ (the vertical plate) has been solved analytically by Ursell;[7] comparison of our results (with $N = 15$) with his shows excellent agreement. Also, in this configuration, the behaviour of $|\mathscr{R}|$ increasing to $|\mathscr{R}| = 1$ monotonically as Ka increases is observed. However, for $M \neq 0$ we find that $|\mathscr{R}|$ increases to $|\mathscr{R}| = 1$ for a finite value of Ka, and then reduces before increasing again. It is noteworthy that, as M increases, total reflection is reached more quickly and the subsequent reduction occurs more rapidly.

Figure 9 continues to follow this behaviour (with $N = 20$) as θ is increased further towards $\pi/2$. We see a pattern emerging, whereby the points of total reflection become more concentrated towards $Ka = 0$, and take on a notably spiked behaviour. This behaviour becomes more pronounced as $\theta \to \pi/2$.

Figure 10 contains two curves. One is the graph of $|\mathscr{R}|$ against Ka for $\theta \approx 98{\cdot}7\%$ of $\pi/2$ (with $N = 30$). We see a striking behaviour, with spikes giving rise to complete reflection, but also an underlying smooth curve throughout the range of Ka. We postulate that the smooth underlying curve is the solution to the dock problem (where the plate lies *in* the free surface) and that

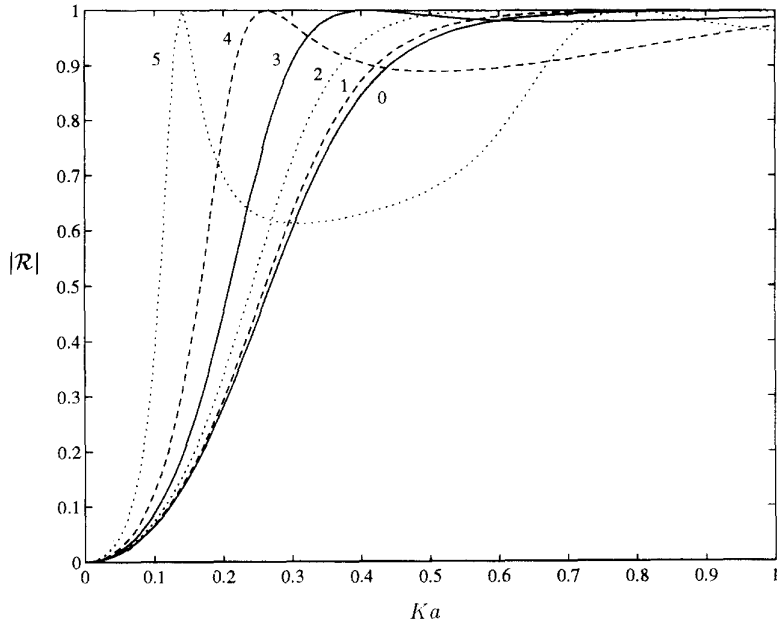

Fig. 8. Graphs of $|\mathscr{R}|$ against Ka, for $\theta = M\pi/12$ and $M = 0, 1, 2, 3, 4$ and 5, where θ is the angle made by the plate to the vertical.

the spikes are due to quasi-resonance of the narrow fluid wedge trapped above the plate. This is illustrated by the second curve in Fig. 10, which is a graph of $|\mathscr{R}|$ for the finite dock, obtained by solving a well-known Fredholm integral equation of the second kind (with a logarithmic kernel) for the boundary values of ϕ_{sc} on the dock.[14,20] It should be possible to analyse this behaviour, asymptotically; such an analysis has been given by Kriegsmann *et al.*[21] for some acoustic problems which give rise to similar behaviour. Finally, we note a fundamental difference, which can be seen from this and the earlier results, between scattering by submerged plates and by surface-piercing plates. As $Ka \to \infty$, waves become confined to an ever smaller region near the free surface, therefore the reflection coefficient for a submerged plate will *always* approach zero in this limit because the plate will become invisible to the waves. However, a surface-piercing plate will *never* become invisible to a surface wave and, moreover, as $Ka \to \infty$ the wave will be unable to reach down far enough to pass under the plate thereby giving rise to complete reflection in this same limit.

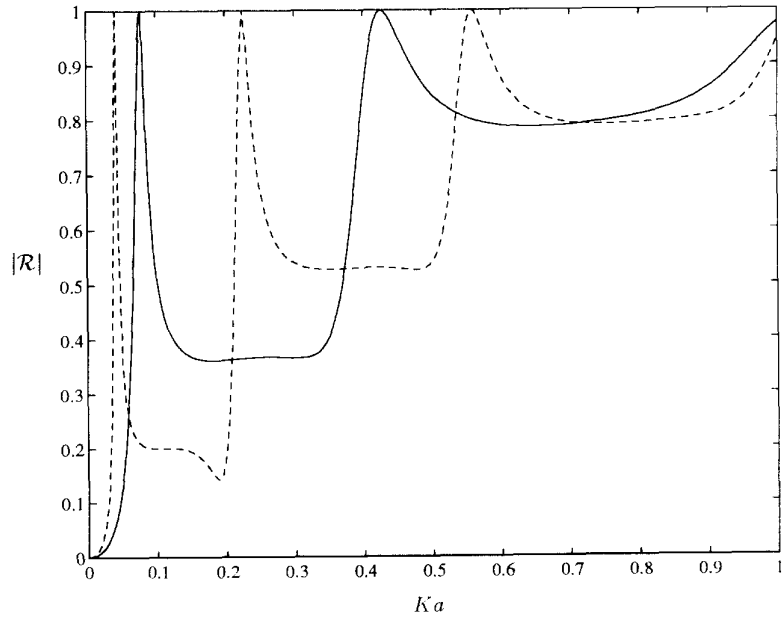

Fig. 9. Graphs of $|\mathscr{R}|$ against Ka, for $\theta = 22\pi/48$ (—) and $23\pi/48$ (– –), where θ is the angle made by the plate to the vertical.

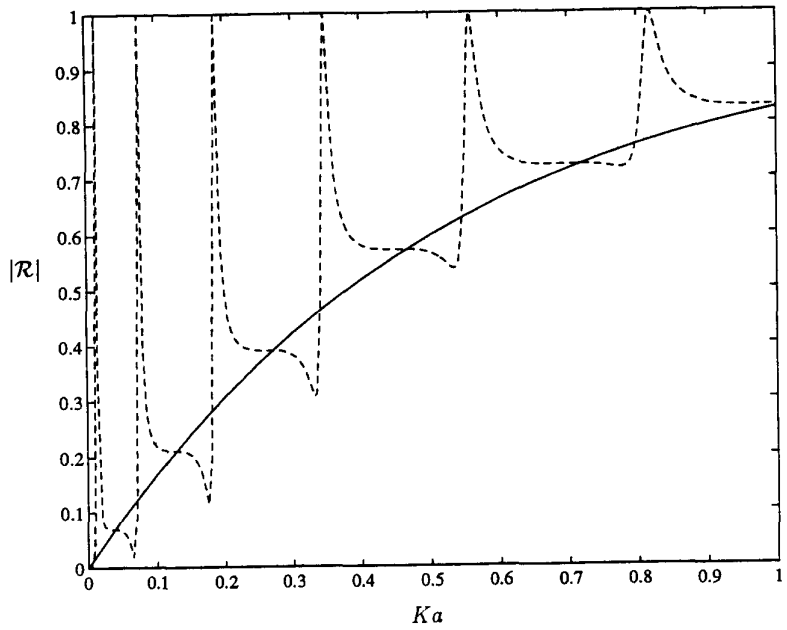

Fig. 10. Graph of $|\mathcal{R}|$ against Ka for the finite dock (—), together with the graph of $|\mathcal{R}|$ against Ka for the surface-piercing flat plate (– –) whose submerged end is rotated so that the plate is almost lying in the free surface ($\theta \approx 98{\cdot}7\%$ of $\pi/2$, where θ is the angle made by the plate to the vertical).

ACKNOWLEDGEMENTS

NFP was supported by a studentship from the SERC.

REFERENCES

1. Parsons, N. F. & Martin, P. A. Scattering of water waves by submerged plates using hypersingular integral equations. *Appl. Ocean Res.*, **41** (1992) 313–21.
2. Evans, D. V. Diffraction of water-waves by a submerged vertical plate. *J. Fluid Mech.*, **40** (1970) 433–51.
3. Patarapanich, M. Forces and moments on a horizontal plate due to wave scattering. *Coastal Engng*, **8** (1984) 279–301.
4. McIver, M. Diffraction of water waves by a moored, horizontal, flat plate. *J. Engng. Math.*, **19** (1985) 297–319.
5. Dean, W. R., On the reflexion of surface waves by a submerged, circular cylinder. *Proc. Camb. Phil. Soc.*, **44** (1948) 483–91.
6. Ursell, F. Surface waves on deep water in the presence of a submerged circular cylinder. I. *Proc. Camb. Phil. Soc.*, **46** (1950) 141–52.
7. Ursell, F. The effect of fixed vertical barrier on surface waves in deep water. *Proc. Camb. Phil. Soc.*, **43** (1947) 374–82.
8. Martin, P. A. & Rizzo, F. J. On boundary integral equations for crack problems. *Proc. Roy. Soc. A*, **421** (1989) 341–55.
9. Yu, Y.S. & Ursell, F. Surface waves generated by an oscillating circular cylinder on shallow water: theory and experiment. *J. Fluid Mech.*, **11** (1961) 529–51.
10. Martin, P. A. End-point behaviour of solutions to hypersingular integral equations. *Proc. Roy. Soc. A*, **432** (1991) 301–20.
11. Golberg, M. A. The convergence of several algorithms for solving integral equations with finite-part integrals. *J. Integ. Eqns*, **5** (1983) 329–40.
12. Golberg, M. A. The convergence of several algorithms for solving integral equations with finite-part integrals. II. *J. Integ. Eqns*, **9** (1985) 267–75.
13. Ervin, V. J. & Stephan, E. P. Collocation with Chebyshev polynomials for a hypersingular integral equation on an interval. *J. Comp. Appl. Math.*, **43** (1992) 221–9.
14. Parsons, N. F. The Interaction of Water Waves with Thin Plates. Ph.D. thesis, University of Manchester, Manchester, UK, 1994.
15. John, F. Waves in the presence of an inclined barrier. *Comm. Appl. Math.*, **1** (1948) 149–200.
16. Liu, P. L. F. & Abbaspour, M. Wave scattering by a rigid thin barrier. *J. Waterway, Port, Coastal and Ocean Div.*, ASCE, **108** (1982) 479–91.
17. Hamilton, W. S. Forces exerted by waves on a sloping board. *Trans. Am. Geophys. Union*, **31** (1950) 849–55.
18. Stoker, J. J. *Water Waves*. Interscience, New York, 1957.
19. Ursell, F. Trapping modes in the theory of surface waves. *Proc. Camb. Phil. Soc.*, **47** (1951) 347–58.
20. MacCamy, R. C. On the heaving motion of cylinders of shallow draft. *J. Ship Res.*, **5**(3) (1961) 34–43.
21. Kriegsmann, G. A., Norris, A. N. & Reiss, E. L. Scattering by penetrable acoustic targets. *Wave Motion*, **6** (1984) 501–16.